Available online at www.sciencedirect.com
SCIENCE DIRECT®
Journal of Computational Physics 185 (2003) 583–611
JOURNAL OF COMPUTATIONAL PHYSICS
www.elsevier.com/locate/jcp

On balanced approximations for time integration of multiple time scale systems

D.A. Knoll [a,*], L. Chacon [a], L.G. Margolin [b], V.A. Mousseau [a]

[a] *Theoretical Division, Los Alamos National Laboratory, Los Alamos, NM 87545, USA*
[b] *Applied Physics Division, Los Alamos National Laboratory, Los Alamos, NM, 87545 USA*

Received 22 April 2002; received in revised form 4 December 2002; accepted 30 December 2002

Abstract

The effect of various numerical approximations used to solve linear and nonlinear problems with multiple time scales is studied in the framework of modified equation analysis (MEA). First, MEA is used to study the effect of linearization and splitting in a simple nonlinear ordinary differential equation (ODE), and in a linear partial differential equation (PDE). Several time discretizations of the ODE and PDE are considered, and the resulting truncation terms are compared analytically and numerically. It is demonstrated quantitatively that both linearization and splitting can result in accuracy degradation when a computational time step larger than any of the competing (fast) time scales is employed. Many of the issues uncovered on the simple problems are shown to persist in more realistic applications. Specifically, several differencing schemes using linearization and/or time splitting are applied to problems in nonequilibrium radiation–diffusion, magnetohydrodynamics, and shallow water flow, and their solutions are compared to those using balanced time integration methods.

1. Introduction

The simulation of complex physical processes with multiple time scales presents a continuing challenge to the numerical modeler due to the co-existence of fast and slow time scales. The multiple time scale system is termed stiff if it contains both fast and slow time scales. In situations where the fast time scales are important, one must either resolve them (i.e., with a small time step) or model their effects. Often, however, the details of the fast time scales are not important. These are situations in which there exists a near balance among the various processes, and the dynamical time scale of the overall evolution is slow. Mathematically, these situations are often described by dissipative, nonlinear partial differential equations (PDEs) that imply the existence of a compact global attractor and an enslaving of the fast scales. It is this class of multiple time

* Corresponding author. Tel.: +1-505-667-7467; fax: +1-505-665-5926.
E-mail address: nol@lanl.gov (D.A. Knoll).

0021-9991/03/$ - see front matter
doi:10.1016/S0021-9991(03)00008-1

scale problems that we address in this paper. There are many examples of such problems in plasma physics, geophysical fluid dynamics, combustion, and radiation hydrodynamics; see, e.g. [1].

For such problems, it is desirable (from the point of view of computational efficiency) to resolve only the dynamical (slow) time scales. However, this requires overstepping the fast time scales while preserving the dynamical balance responsible for the time scale enslavement. One effective way to achieve this is by designing nonlinear, implicit difference schemes in which a consistent solution of the separate processes is ensured even when large time steps (of the order of the dynamical time scale) are employed. We will refer to such techniques as being implicitly balanced.

Implicitly balanced schemes have been avoided in the past due to the lack of efficient implicit solvers. Instead, formulations based on time-splitting and/or linearization have predominated. However, recent progress in developing effective preconditioners is making Jacobian-free Newton–Krylov methods [2,3] a viable choice for many multiple time scale problems.

The classical analysis of splitting and linearization errors is based on asymptotic expansions of exponential operators – see [4–6]. This technique is well-suited to determine stability and to assess the order of accuracy (i.e., rate of convergence) of these algorithms, and the results in [5,6] also support the use of implicitly balanced methods for multiple time scale problems. However, this analysis is less useful for quantitatively estimating the consequences of linearization, the effects of boundary conditions, or the error itself. These latter can be more readily diagnosed using an alternate technique known as modified equation analysis (MEA) [7–9].

The goals of this paper are twofold. First, we will demonstrate the use of MEA to analyze and estimate linearization and splitting errors. We will use simple examples to show that, even when numerically stable for arbitrary time steps, linearization and splitting can alter the dynamical balance of the modeled system, a result of additional truncation terms that degrade numerical accuracy. We will further demonstrate that MEA can be used to identify these additional truncation terms. Second, we will illustrate the ability of implicitly balanced algorithms to maintain accuracy while resolving only the dynamical time scale in a suite of practical applications described by nonlinear, coupled sets of PDEs, including 1D nonequilibrium radiation–diffusion, 2D magnetohydrodynamics, and the 2D shallow water flows. We will compare the accuracy of implicitly balanced methods with that of split and/or linearized methods. We will show that, for a given level of error, implicitly balanced methods allow larger time steps (in some cases, orders of magnitude larger) than those required by split and/or linearized methods. Finally, owing to space limitations, we can not consider all possible splitting or linearization time integration methods. In this manuscript we consider first-order methods, as these methods are in use in a wide variety of large scale simulation codes. Future work will consider higher-order splitting and linearization, some of which is underway [10].

The remainder of the paper is organized as follows. In Section 2, we discuss the concepts of MEA, asymptotic balance, and implicitly balanced methods. In Section 3, we use MEA to study the numerical consequences of linearization in a simple ODE, and to study the numerical consequences of splitting in a linear reaction–diffusion PDE. In Section 4, we demonstrate advantages of implicitly balanced methods in practical applications. Finally, we summarize our results in Section 5.

2. Background

2.1. Modified equation analysis

Modified equation analysis (MEA) is often used in computational physics to assess the stability and accuracy of numerical algorithms. The modified equation results from a Taylor series expansion of the discrete fields of the algorithm, treated as if they were continuous. For a consistent algorithm, the modified equation is the original PDE augmented by the lowest-order truncation terms, i.e., terms whose coefficients

contain discretization parameters such as the time step or computational cell size. For a consistent discretization, truncation terms vanish as the discretization parameters tend to zero. However, in practice these parameters always remain finite, and so the underlying idea is that the modified equation describes the behavior of the discrete equations more accurately than the original PDE.

MEA was originally used to assess the computational stability of nonlinear equations for which the standard Fourier techniques cannot be applied [7]. Warming and Hyett [8] established a formal connection between the standard Fourier techniques and MEA, and pointed out the importance of using the discretized equations consistently, rather than the original PDE, in the derivation of the modified equation. Griffith and Sanz-Serna [9] provide an excellent review of the technique and emphasize the importance of considering the "modified problem" – i.e., the modified equations supplemented by the necessary initial and boundary conditions. Chang [11] noted an additional issue, that MEA applied to multiple time level algorithms may not identify all sources of instability in the algorithm.

MEA has been used in the construction of high-resolution advection algorithms. For example in [12], MEA is employed to identify the second-order errors in donor cell differencing, which are then compensated to increase the order of accuracy of the scheme. This process can then be repeated in the revised algorithm, to identify and compensate third-order errors. MEA has also been used to identify and reduce specific splitting errors that arise when advective terms and the forcing terms in the momentum equation are treated separately [13]. MEA has recently been applied to study spatial discretization schemes being developed to more accurately simulate problems with multiple spatial scales [14].

Finally, we note an additional caveat in the use of MEA for multiple time scale systems. A Taylor series is an expansion in a small parameter. In this context, small must be judged in terms of dimensionless parameters. For expansions in time, the parameter typically will be the ratio of the computational time step to a physical time scale. A subtle pitfall can arise in problems where several fast processes compete to yield a slower dynamical time scale. In such situations, one can not assume that all time-dependent quantities evolve on the (slow) dynamical time scale, since individual terms in the equations may depend on the fast time scales. This is particularly relevant when considering "accurate" Taylor expansions of the separate terms if the time step is larger than the fastest time scales in the system. Thus, MEA must be applied to multiple time scale problems with caution.

2.2. Asymptotic balance and enslavement

The evolution of many physical systems is described by nonlinear dissipative PDEs. For example, in continuum mechanics, nonlinearity naturally appears in the convective terms, while essentially all realizable physical systems are dissipative. An asymptotic property of certain such PDEs is the development of an approximate balance between the nonlinear and the dissipative terms. This balance, coupled with the nonlinearity of the equations, leads to enslavement wherein the small scales of motion are organized (i.e., enslaved) by the large scales. The balance also implies that the tendency terms (time derivatives) are small. That is, the overall dynamical time scale is much larger than the smaller time scales of the individual processes (i.e., normal modes).

Because the system evolves on a slower time scale, it is not necessary to resolve the fast time scales so long as the numerical approximations accurately preserve the asymptotic balance. In the context of Galerkin methods, a technique known as the approximate inertial manifold (AIM; see [15]) directly employs the enslavement to preserve the balance. A related technique has been developed for explicit finite difference/volume methods [16]; termed nonlinear enslavement, these algorithms essentially condition the truncation error to enforce the balance. The enslavement techniques have also been applied successfully to systems in which dissipation is not part of the principal balance, although there is not yet any formal mathematical justification [17]. AIM and enslavement techniques require an explicit construction of the

relation between fast and slow time scales (i.e., the inertial manifold), and so can be difficult to apply to complex systems with many interacting processes.

2.3. Implicitly balanced methods

We are interested in multiple time scale problems where the dynamical time scale is much slower than one or more of the normal mode time scales. Since we desire time steps that are larger than the normal mode time scales, we require implicit methods. In addition, we desire that our time integration approach strike the correct asymptotic balance on the dynamical time scale. Let us discuss what we mean by an implicitly balanced approximation. Consider an evolution equation for a variable $T(x,t)$ that can be written abstractly in the form

$$\frac{\partial T}{\partial t} = R(T) + D(T), \tag{1}$$

where R and D are nonlinear operators acting on T and its spatial derivatives. We define the dynamical time scale, τ_{dyn}, by

$$\tau_{\mathrm{dyn}} \equiv \left(\left| \frac{1}{T} \frac{\partial T}{\partial t} \right| \right)^{-1}. \tag{2}$$

The time scales associated with the process represented by R and D (normal modes) may be fast compared to the dynamical time scale. In many problems of interest the slower dynamical time scale is a result of a near balance between R and D. An implicitly balanced approximation to this equation is

$$\frac{T^{n+1} - T^n}{\Delta t} = R(T^*) + D(T^*), \tag{3}$$

where $T^* \equiv T(x,t^*)$, and Δt is the computational time step. What makes this approximation implicitly balanced is that the both operators are evaluated at the same instant of time, $t^* \in [t^n, t^{n+1}]$.

In this study we employ methods that are implicitly balanced and that are both first- and second-order accurate in time. We do not consider all possible methods that could be referred to as implicitly balanced. It is our premise that the practices of time splitting and linearization have the potential to numerically compromise the natural asymptotic balance of a multiple time scale system. In this study we demonstrate how this can happen.

Implicit formulations (the method of choice in this work) are well-suited to maintain the asymptotic balance in complex multiple time scale problems, because all relevant terms in the PDE system can be approximated at the same time level. However, implicit algorithms of nonlinear PDEs require the solution of nonlinear algebraic equations. Jacobian-free Newton–Krylov techniques allow one to efficiently solve the nonlinear system of algebraic equations $\vec{G}(\vec{x}) = 0$, resulting from an implicit discretization of a system of nonlinear PDEs. The nonlinear terms are converged using a Newton–Raphson iterative scheme, which requires the inversion of the Jacobian system $J_m \delta\vec{x}_m = -\vec{G}(\vec{x}_m)$, where $J_m = \partial\vec{G}/\partial\vec{x}|_m$ is the Jacobian matrix and $\vec{G}(\vec{x}_m)$ is the nonlinear residual at each Newton iteration level m. The updated solution is $\vec{x}_{m+1} = \vec{x}_m + \delta\vec{x}_m$, and the iteration proceeds until $||\vec{G}(\vec{x}_{m+1})|| < \epsilon_{\mathrm{a}} + \epsilon_{\mathrm{r}}||\vec{G}(\vec{x}_0)||$, where $\vec{G}(\vec{x}_m)$ has been properly nondimensionalized. Here ϵ_{a} and ϵ_{r} are an absolute and a relative tolerance, respectively. The required matrix inversions are performed iteratively using Krylov methods (typically, GMRES [18] for nonsymmetric, indefinite systems), which allow a Jacobian-free implementation [2,3] (i.e., in which the Jacobian is neither formed or stored), and preconditioning [18]. The preconditioner is based on reformulating the Jacobian system as $JP^{-1}P\delta\vec{x} = \vec{G}$ (right preconditioning), where P^{-1} approximates the Jacobian inverse in some (inexpensive) way. In practice, one solves for $\vec{r}$ from $JP^{-1}\vec{r} = \vec{G}$, and then the Newton

update is found from $\delta\vec{x} = P^{-1}\vec{r}$. The preconditioning step effectively improves the condition number of the system, and can be seamlessly implemented in the Krylov algorithm.

Formulating an effective and inexpensive preconditioner is essential to achieve efficiency in the Krylov iteration, and is the focus of intense ongoing research in a variety of physical applications. In particular, the preconditioning strategies for the applications used in Section 4 are described in detail in [19–21]. In all cases, the preconditioners have been constructed from non-Newton linearized and/or split methods. These preconditioners do not effect the accuracy of the Newton–Krylov methods, only their efficiency.

3. Model problems

In this section, we will consider the practices of linearization and splitting within the context of a nonlinear reaction–diffusion model problem

$$\frac{\partial T}{\partial t} - D\frac{\partial^2 T}{\partial x^2} = \alpha(T)T, \tag{4}$$

where T is the dependent variable (e.g., temperature), D is a diffusion coefficient, and $\alpha(T)$ is a reaction coefficient. For brevity, and to relate to the results in Section 4, we will consider a nonlinear reaction problem (an ODE) and a linear reaction–diffusion problem (a PDE).

3.1. Nonlinear reaction

Setting the diffusion coefficient to zero in Eq. (4) produces the nonlinear ordinary differential equation (ODE)

$$\frac{\mathrm{d}T}{\mathrm{d}t} = \alpha(T)T. \tag{5}$$

Here the dynamical time scale is

$$\tau_{\mathrm{dyn}} \equiv \left|\frac{1}{T}\frac{\mathrm{d}T}{\mathrm{d}t}\right|^{-1} = |\alpha|^{-1}. \tag{6}$$

The time scale governing the characteristic rate of change of α is

$$\tau_\alpha \equiv \left|\frac{1}{\alpha}\frac{\mathrm{d}\alpha}{\mathrm{d}t}\right|^{-1}. \tag{7}$$

It is possible that $\tau_\alpha < \tau_{\mathrm{dyn}}$, and this is the situation that we consider.

We employ three time discretizations: a first-order accurate nonlinear method (backward Euler)

$$\frac{T^{n+1} - T^n}{\Delta t} = \alpha(T^{n+1})T^{n+1}, \tag{8}$$

a second-order accurate nonlinear method (trapezoidal rule)

$$\frac{T^{n+1} - T^n}{\Delta t} = \frac{1}{2}\left(\alpha(T^{n+1})T^{n+1} + \alpha(T^n)T^n\right), \tag{9}$$

and a first-order method, where α is linearized at the previous time level

$$\frac{T^{n+1}-T^n}{\Delta t}=\alpha(T^n)T^{n+1}. \tag{10}$$

(It is possible for this linearized method to be second order.) The practice of linearizing nonlinear coefficients at the previous time level is common [22,23], and it is often referred to as a semi-implicit (SI) approach [19].

To perform the MEA on these discretizations, we will use a truncated Taylor series expansion in time of the temperature; for example

$$T^n=T^{n+1}-\Delta t T_t^{n+1}+\frac{\Delta t^2}{2}T_{tt}^{n+1}-\frac{\Delta t^3}{6}T_{ttt}^{n+1}+\mathrm{O}(\Delta t^4). \tag{11}$$

This expansion is assumed to be accurate on the dynamical time scale, $\Delta t<\tau_{\mathrm{dyn}}$. (We use the shorthand notation $T_t\equiv \mathrm{d}T/\mathrm{d}t$, etc.) We will also use a truncated Taylor series expansion of the reaction coefficient,

$$\alpha^n=\alpha^{n+1}-\Delta t\frac{\mathrm{d}\alpha^{n+1}}{\mathrm{d}t}+\frac{\Delta t^2}{2}\frac{d^2\alpha^{n+1}}{dt^2}+\mathrm{O}(\Delta t^3). \tag{12}$$

This expansion will be accurate for $\Delta t<\tau_\alpha$, which again may be smaller than τ_{dyn}.

It is understood that any time integration method can fail to produce its design, or asymptotic, convergence rate if the time step is too large. It is also understood that when this occurs, it is a result of higher-order terms in the Taylor series expansion becoming important. The primary goal of this subsection is to demonstrate that when Eq. (8) fails to produce its asymptotic convergence rate, it is a result of higher-order terms in the expansion of T, whereas when Eq. (10) fails to produce its asymptotic convergence rate, it is a result of higher-order terms in the expansion of α.

After performing the MEA and moving the leading order errors to the right-hand side, we derive the modified equation for the first-order nonlinear method (Eq. (8))

$$[T_t-\alpha(T)T]=\frac{\Delta t}{2}T_{tt}+\mathrm{O}(\Delta t^2). \tag{13}$$

The modified equation for the second-order nonlinear method (Eq. (9)) is

$$[T_t-\alpha(T)T]=\frac{\Delta t^2}{24}T_{ttt}+\mathrm{O}(\Delta t^3). \tag{14}$$

Finally, the modified equation for the first-order linearized method (Eq. (10)) is

$$[T_t-\alpha(T)T]=\frac{\Delta t}{2}T_{tt}-\underline{\frac{\mathrm{d}\alpha}{\mathrm{d}t}\Delta tT}+\mathrm{O}(\Delta t^2). \tag{15}$$

Note that in constructing the modified equation for the linearized method Eq. (15), we have assumed that a first-order expansion of α is adequate (although, as noted in Section 2.1, it may be necessary to include higher-order terms in the Taylor expansion of $\alpha(T)$ depending on the time step size). In general, when we use the notation $\mathrm{O}(\Delta t^2)$ we are assuming that Δt is such that all higher-order terms (second and above) make small contributions to the expansion.

Analysis of these modified equations allows us to identify the sources of numerical error and, in some situations, to devise more accurate discretizations. For instance, as compared to the modified equation of the first-order nonlinear method (Eq. (13)), the modified equation of the linearized method (Eq. (15)) has an additional first-order truncation term that is proportional to $(\mathrm{d}\alpha/\mathrm{d}t)T$ (underlined term). This recognition can be used to define an "effective" reaction rate $\alpha^*=\alpha(T)+(\mathrm{d}\alpha/\mathrm{d}t)\Delta t$ that, when employed with the linearized method (Eq. (10)), recovers the solution of the nonlinear method (Eq. (8)). Conversely, using the first-order nonlinear method to solve

$$[T_t - \alpha(T)T] = \left(-\frac{\mathrm{d}\alpha}{\mathrm{d}t}\Delta t \right) T, \tag{16}$$

should reproduce the solution given by the linearized discretization (Eq. (10)). [Note that the first-order time integration will reproduce the truncation term $(\Delta t/2)T_{tt}$ in Eq. (15).] When the first-order Taylor series expansion in α is not adequate (e.g., $\Delta t > \tau_\alpha$), then a first-order nonlinear solution of

$$[T_t - \alpha(T)T] = \left(-\frac{\mathrm{d}\alpha}{\mathrm{d}t}\Delta t + \frac{\mathrm{d}^2\alpha}{\mathrm{d}t^2}\frac{\Delta t^2}{2} \right) T, \tag{17}$$

may more accurately reproduce the linearized method solution since it accounts for the second term in the expansion of α. When this is the case then we should not expect the linearized method to produce first-order time step convergence.

Similarly, a higher-order (second or above) solution of

$$[T_t - \alpha(T)T] - \frac{\Delta t}{2} T_{tt} = 0, \tag{18}$$

will reproduce the solution of Eq. (8) as long as the first-order truncation of Eq. (11) is accurate. If this is not the case then a higher-order solution of

$$[T_t - \alpha(T)T] - \frac{\Delta t}{2} T_{tt} + \frac{\Delta t^2}{12} T_{ttt} = 0, \tag{19}$$

will most likely do better. Again, at this point we would not expect the first-order nonlinear method (Eq. (8)) to produce first-order time step convergence. The main point here is that the accuracy of the Taylor series expansion of T controls the design accuracy (convergence rate) of the nonlinear method, while that of the Taylor series expansion of α controls the design accuracy (convergence rate) of the linearized method.

We now illustrate this discussion by choosing a particular form for the reactivity $\alpha(T)$, and comparing the solutions using the first-order linearized algorithm, the first- and second-order nonlinear algorithms, and the solutions resulting from using the first-order nonlinear algorithm to solve Eqs. (16) and (17). We choose $\alpha(T) = -(T^3 + a)^{-1}$ with $T(0) = 1.0$. The constant a bounds α as $T \to 0$; we use $a = 2.0 \times 10^{-2}$. Then

$$\frac{\mathrm{d}\alpha}{\mathrm{d}T} = \frac{3T^2}{(T^3 + a)^2}, \tag{20}$$

and

$$\frac{\mathrm{d}^2\alpha}{\mathrm{d}T^2} = \frac{6T(a - 2T^3)}{(T^3 + a)^3}. \tag{21}$$

Figs. 1–3 show the solutions for the second-order nonlinear method, the first-order nonlinear method and the first-order linearized method, respectively. The baseline solution is obtained with the second-order nonlinear method using a small time step to ensure accuracy. The dynamical time scale τ_{dyn} (Eq. (6)) is a function of time, and is smallest at $t = 0.35$, where $\tau_{\mathrm{dyn}} \approx 4.0 \times 10^{-2}$. The nonlinear second-order method retains accuracy even when using time steps $\Delta t = 2.0 \times 10^{-2} \approx \tau_{\mathrm{dyn}}$ – cf. Fig. 1. However, as illustrated in Figs. 2 and 3, the first-order nonlinear method and the linearized method clearly require a smaller time step to achieve the same level of accuracy.

To determine when a first-order Taylor expansion of α fails to be sufficiently accurate, we compare Eqs. (16) and (17) solved with a first-order nonlinear method to the solution of the linearized method. In Fig. 4

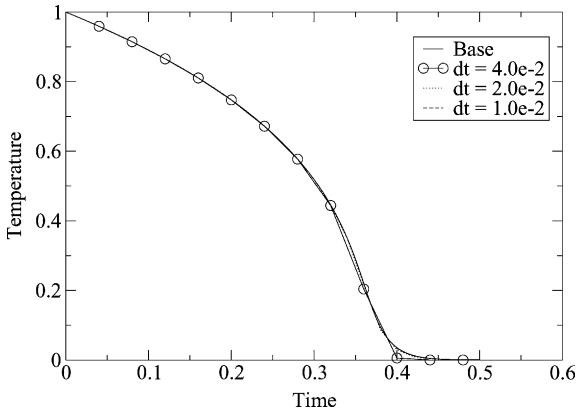

Fig. 1. Performance of the second-order nonlinear method on the nonlinear reaction problem.

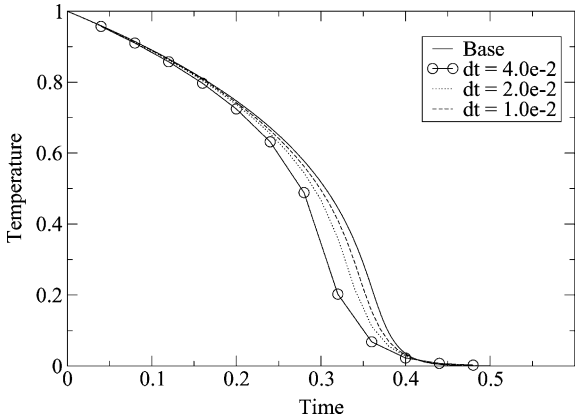

Fig. 2. Performance of the first-order nonlinear method on the nonlinear reaction problem.

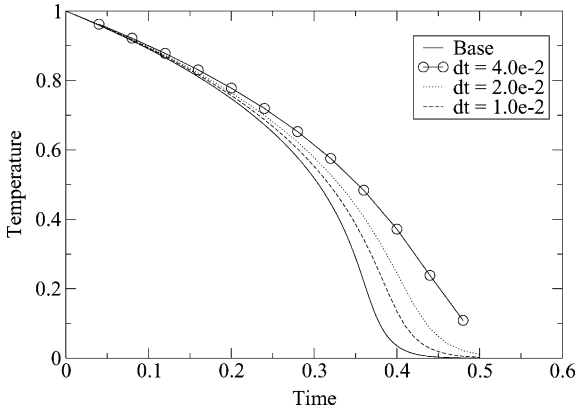

Fig. 3. Performance of the first-order linearized method on the nonlinear reaction problem.

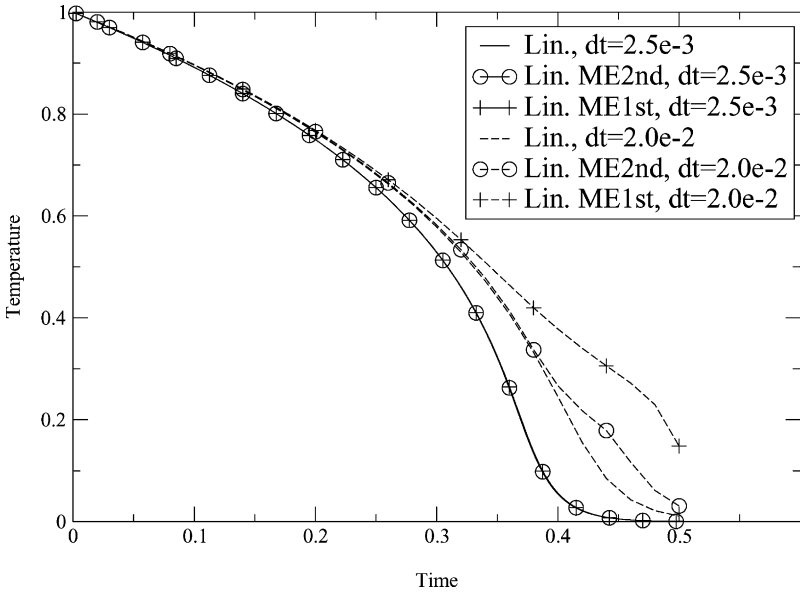

Fig. 4. Comparison of the first-order linearized solution and its modified equation with first- and second-order Taylor expansions for two different time steps ($\Delta t = 0.0025,\ 0.02$).

one can see comparisons of solutions for two choices of time step. Each comparison contains three solutions: (1) the linearized method; (2) the first-order nonlinear solution of Eq. (16); (3) the first-order nonlinear solution of Eq. (17). At the smaller time step ($\Delta t < \tau_\alpha$), all three solutions are equivalent, demonstrating that the modified equation with a first-order expansion in α is sufficient. For time steps comparable or less than this value, we should expect first-order convergence of the linearized method. At a larger time step ($\Delta t \approx \tau_\alpha$), the result is quite different. Here the second-order expansion of α provides a noticeably better approximation to the linearized solution. For this larger time step, the first-order expansion in α is not adequate, and we should not expect first-order convergence. To emphasize this point, we plot

$$\frac{\Delta t}{\alpha}\frac{\mathrm{d}\alpha}{\mathrm{d}t} \quad \text{and} \quad \frac{\Delta t^2}{2\alpha}\frac{\mathrm{d}^2\alpha}{\mathrm{d}t^2}$$

for $\Delta t = 2.0 \times 10^{-3}$ and $\Delta t = 1.0 \times 10^{-2}$ in Fig. 5. These are the first two terms in the Taylor series for α (Eq. (12)) normalized by α. At about time $= 0.34$, $\Delta t = 2.0 \times 10^{-3}$, the first term is about 0.08 while the second term is about 0.004. Thus the second term is less then 1% of the total and only 5% of the first term. At the same point in time, but with $\Delta t = 1.0 \times 10^{-2}$, the first term is about 0.54 while the second term is now 0.12. Thus the second term is greater than 10% of the total and about 20% of the first term.

The effect of the inaccurate Taylor expansion on the numerical solution error is evident in Fig. 6, which depicts the results of a convergence study as a function of time step. While the second-order method exhibits uniform second-order convergence, the linearized method exhibits first-order convergence only at small time steps. In Fig. 7 we display the results of a time step convergence study for the two first-order methods. At some time step, each method loses first-order convergence. The nonlinear method is the more accurate, and retains first-order convergence to a larger time step. The behavior of the first-order nonlinear method can be understood by considering the Taylor series expansion of T. Fig. 8 is the companion plot to Fig. 5, but now we plot the first- and second-order terms in Eq. (11) normalized by T. At time $= 0.34$, and

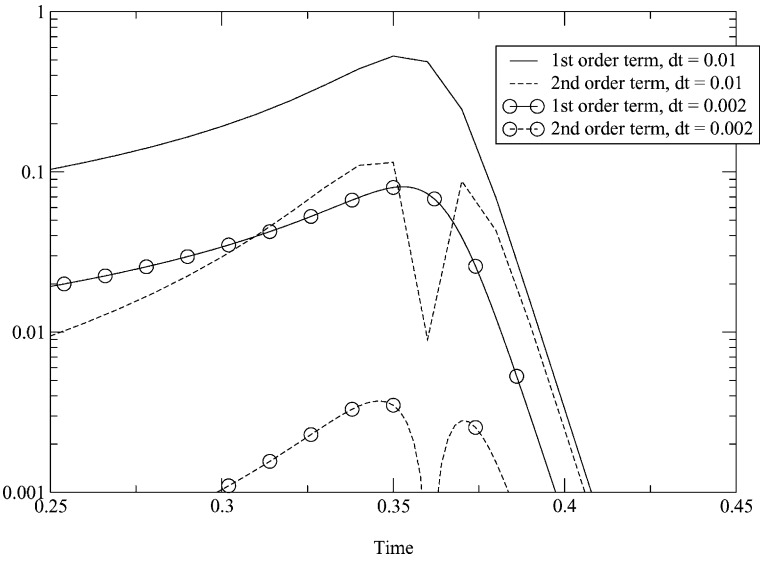

Fig. 5. Plot of $\frac{\Delta t}{\alpha}\frac{d\alpha}{dt}$ and $\frac{\Delta t^2}{2\alpha}\frac{d^2\alpha}{dt^2}$ for two different time steps ($\Delta t = 0.002,\ 0.01$).

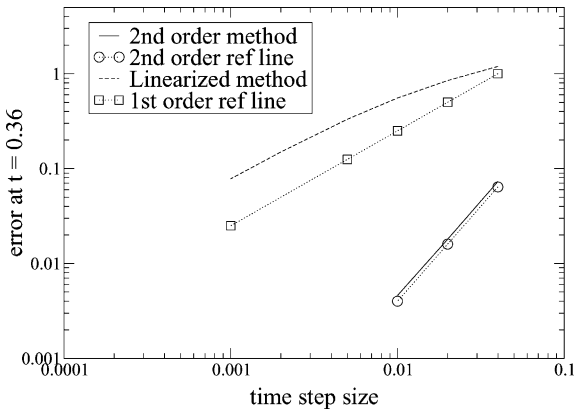

Fig. 6. Time step convergence study of the first-order linearized method and the second-order nonlinear method for the nonlinear reaction problem.

$\Delta t = 1.0 \times 10^{-2}$, the first-order term is about 0.2 while the second-order term is still about 0.01. Thus the second-order term is 1% of the total and only 5% of the first-order term.

This explains why the first-order nonlinear method maintains first-order time step convergence at a larger time step as compared to the first-order linearized method. The gap in time step is not large for this model problem, but large enough to establish the concept. Again, achieving the design convergence rate with the nonlinear method depends on the accuracy on the Taylor expansion of T, while achieving the design convergence rate with the linearized method depends on that of the expansion of α.

3.2. Linear reaction–diffusion

Next we apply MEA to analyze the effects of time splitting. We only consider the simplest first-order splittings to illustrate the technique. We recognize that it is straightforward to design a second-order ac-

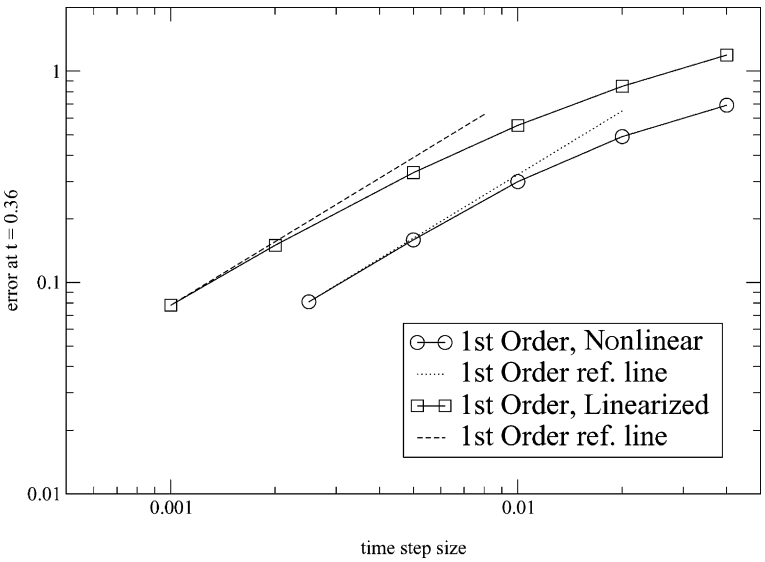

Fig. 7. Time step convergence study of the first-order linearized method and the first-order nonlinear method for the nonlinear reaction problem.

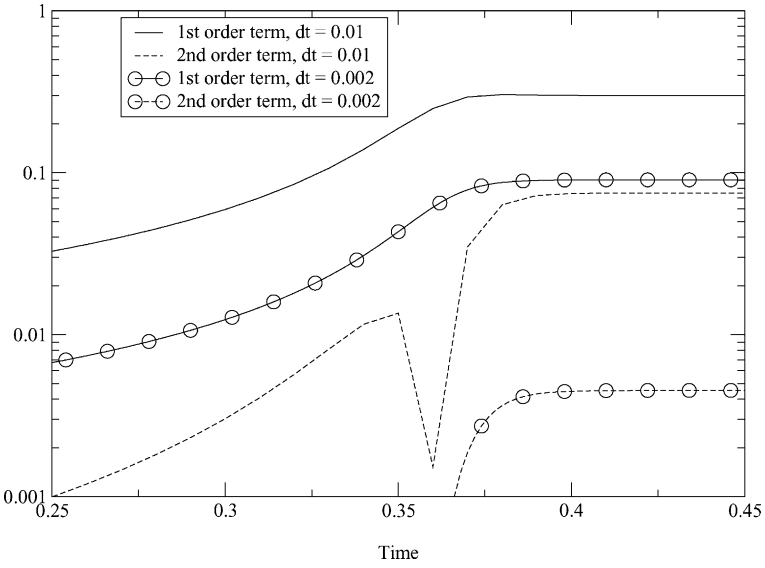

Fig. 8. Plot of $\frac{\Delta t}{T}\frac{dT}{dt}$ and $\frac{\Delta t^2}{2T}\frac{d^2T}{dt^2}$ for two different time steps ($\Delta t = 0.002,\ 0.01$).

curate splitting for the problem considered below. Second-order splittings have been applied to the non-equilibrium radiation–diffusion problem of Section 4.1 in [10]. In that work it was shown that second-order split methods can produce large errors, as compared to second-order implicitly balanced methods, when the time step approaches the dynamical time scale. MEA analysis of more sophisticated splittings will be undertaken in a future study. Here, we consider the linear reaction–diffusion problem (Eq. (4)) with a constant diffusivity D and constant reactivity $\alpha < 0$

$$\frac{\partial T}{\partial t} - D\frac{\partial^2 T}{\partial x^2} = \alpha T, \tag{22}$$

in the domain $0 \leqslant x \leqslant 1$, with boundary and initial conditions

$$T_{x=0} = T_{\mathrm{L}}, \quad T_{x=1} = T_{\mathrm{R}}, \quad T(x, t=0) = 0.$$

The dynamical time scale is estimated as

$$\frac{1}{\tau_{\mathrm{dyn}}} \equiv \left|\frac{1}{T}\frac{\mathrm{d}T}{\mathrm{d}t}\right| \approx \frac{1}{\tau_{\mathrm{dif}}} + \frac{1}{\tau_{\mathrm{reac}}},$$

where

$$\tau_{\mathrm{dif}} \equiv \frac{L^2}{D}, \qquad \tau_{\mathrm{reac}} \equiv \left|\frac{1}{\alpha}\right|,$$

and L is the length of the domain. In general, the diffusion time scale τ_{dif} varies, becoming larger with increasing problem time. This can be seen from the analytic solution of Eq. (22)

$$T(x,t) = T_{\mathrm{SS}}(x) + \sum_{i=1}^{\infty} a_n \mathrm{e}^{-[D(n\pi)^2 - \alpha]t} \sin(n\pi x). \tag{23}$$

Here T_{SS} is the steady-state solution, given by

$$T_{\mathrm{SS}}(x) = \frac{1}{\sinh(1/L_D)}\left[T_{\mathrm{R}} \sinh\left(\frac{x}{L_D}\right) + T_{\mathrm{L}} \sinh\left(\frac{1-x}{L_D}\right)\right],$$

where $L_D^2 = -D/\alpha$, and the Fourier coefficients are defined as

$$a_n = -2\int_0^1 \mathrm{d}x T_{\mathrm{SS}}(s) \sin(n\pi x).$$

From Eq. (23), the dynamical time scale is given by

$$\frac{1}{\tau_{\mathrm{dyn}}} = D(n\pi)^2 + |\alpha|.$$

Hence, $\tau_{\mathrm{dif}} = l_n^2/D$, where $l_n = 1/(n\pi)$ is the characteristic diffusion length scale for each mode n. As time progresses, only modes with longer τ_{dif} (smaller n) survive, and τ_{dif} varies in time accordingly.

3.2.1. Some basics

To solve Eq. (22), we will consider two different first-order time-split methods, one that advances the diffusion first and reaction second (DR), and another that advances the reaction first and diffusion second (RD). Specifically, the first-order RD splitting is:

$$\frac{T^* - T^n}{\Delta t} = \alpha T^*, \quad \frac{T^{n+1} - T^*}{\Delta t} - D\left(\frac{\partial^2 T^{n+1}}{\partial x^2}\right) = 0 \tag{24}$$

and the first-order DR splitting is:

$$\frac{T^* - T^n}{\Delta t} - D\left(\frac{\partial^2 T^*}{\partial x^2}\right) = 0, \quad \frac{T^{n+1} - T^*}{\Delta t} = \alpha T^{n+1}. \tag{25}$$

In both cases T^* is an intermediate, or temporary, value for T. Note that for DR splitting the boundary conditions must be applied to T^*.

We will also consider two balanced methods, one first- and the other second-order accurate in time. The first order, balanced method is

$$\frac{T^{n+1}-T^n}{\Delta t}-D\left(\frac{\partial^2 T^{n+1}}{\partial x^2}\right)=\alpha T^{n+1}, \tag{26}$$

and the second order, balanced method is

$$\frac{T^{n+1}-T^n}{\Delta t}-D\left(\frac{\partial^2 T^{n+(1/2)}}{\partial x^2}\right)=\alpha T^{n+(1/2)}. \tag{27}$$

Here

$$T^{n+(1/2)}\equiv\frac{T^{n+1}+T^n}{2}. \tag{28}$$

As pointed out in [9], it is important to consider the "modified problem", which includes the modified equation, boundary and initial conditions. We will refer to this as modified problem analysis, MPA. In the present example, the modified equation for the two split methods, DR and RD, will be identical, but the modified problems (and in particular the boundary conditions) are different; we will see that this is consistent with the simulation results.

Considering the semi-discrete problem in time (i.e., ignoring the spatial discretization), it is straightforward to show that the modified problem for the first-order unsplit method is

$$\left[T_t-D\left(\frac{\partial^2 T}{\partial x^2}\right)-\alpha T\right]=\frac{\Delta t}{2}T_{tt}+\mathrm{O}(\Delta t^2),\quad T_{x=0}=T_{\mathrm{L}},\ \ T_{x=1}=T_{\mathrm{R}}, \tag{29}$$

and for the second-order unsplit method is

$$\left[T_t-D\left(\frac{\partial^2 T}{\partial x^2}\right)-\alpha T\right]=\frac{\Delta t}{24}T_{ttt}+\mathrm{O}(\Delta t^3),\quad T_{x=0}=T_{\mathrm{L}},\ \ T_{x=1}=T_{\mathrm{R}}. \tag{30}$$

Defining the modified problems for the RD and DR split methods is a bit more subtle.

3.2.2. RD modified problem

After combining the two steps from the RD split method in Eq. (25), we derive

$$\frac{T^{n+1}-T^n}{\Delta t}-D\left(\frac{\partial^2 T^{n+1}}{\partial x^2}\right)=\alpha T^*,\quad T^{n+1}_{x=0}=T_{\mathrm{L}},\ \ T^{n+1}_{x=1}=T_{\mathrm{R}}. \tag{31}$$

To perform the MEA we must eliminate T^n and T^* in favor of T^{n+1} and its time derivatives. As we have seen, T^n can be eliminated using standard Taylor series expansion. Rather than attempting to write a similar Taylor series for T^*, we can use the second step in the RD split method itself,

$$T^*=T^{n+1}-\Delta t D\left(\frac{\partial^2 T^{n+1}}{\partial x^2}\right). \tag{32}$$

The modified problem for the RD splitting method can now be written

$$\left[T_t - D\left(\frac{\partial^2 T}{\partial x^2}\right) - \alpha T\right] = \frac{\Delta t}{2} T_{tt} - \underline{\Delta t \alpha D\left(\frac{\partial^2 T}{\partial x^2}\right)} + \mathrm{O}(\Delta t^2), \quad T_{x=0} = T_{\mathrm{L}}, \;\; T_{x=1} = T_{\mathrm{R}}. \tag{33}$$

As compared with the first-order unsplit method (Eq. (29)), a new first-order truncation term (underlined) has appeared in the RD split modified equation. This new term is proportional to the second spatial derivative, and scales with $\alpha\Delta t$. The modified equation of the RD split method can be identified with the modified equation of the unsplit first-order method using a modified diffusion coefficient. Indeed, if we replace D with D^* in Eq. (33) and equate terms with Eq. (29), we have

$$D^* = \frac{D}{1.0 - \Delta t \alpha}. \tag{34}$$

This suggests that using the RD split algorithm with the diffusion coefficient, D^*, should reproduce the results of the first-order unsplit method with the original diffusion coefficient D. For $\alpha < 0$, the altered diffusion coefficient remains positive and less than the original coefficient.

3.2.3. DR modified problem

We repeat the analysis for the DR split method. After combining the two steps of Eq. (24), we have

$$\frac{T^{n+1} - T^n}{\Delta t} - D\left(\frac{\partial^2 T^*}{\partial x^2}\right) = \alpha T^{n+1}, \quad T^*_{x=0} = T_{\mathrm{L}}, \;\; T^*_{x=1} = T_{\mathrm{R}}. \tag{35}$$

Since the elliptic operator is applied to T^*, our boundary conditions must be enforced for T^*. This is a crucial point in the MPA of the DR splitting. As before, we eliminate T^n using Taylor series expansion and we eliminate T^* using the second step in the DR split method

$$T^* = (1.0 - \Delta t \alpha) T^{n+1}. \tag{36}$$

Then the modified problem is

$$\left[T_t - D\left(\frac{\partial^2 T}{\partial x^2}\right) - \alpha T\right] = \frac{\Delta t}{2} T_{tt} - \underline{\Delta t \alpha D\left(\frac{\partial^2 T}{\partial x^2}\right)} + \mathrm{O}(\Delta t^2), \quad (1 - \underline{\alpha \Delta t}) T_{x=0} = T_{\mathrm{L}}, \quad (1 - \underline{\alpha \Delta t}) T_{x=1} = T_{\mathrm{R}}. \tag{37}$$

We see the same additional first-order truncation term appears in the modified equation for DR as was seen in RD splitting. In addition, DR splitting has introduced an error in the boundary conditions. The MPA shows that the DR splitting is not equivalent to RD splitting *even though their modified equations are identical*, and that for the DR splitting there is an additional new truncation term at the boundary, which scales as $\alpha\Delta t$. In applying the DR split algorithm to this model problem, we could rescale the boundary conditions

$$T^*_{x=0} = T_{\mathrm{L}}/(1 - \alpha\Delta t), \quad T^*_{x=1} = T_{\mathrm{R}}(1 - \alpha\Delta t). \tag{38}$$

Then if we use D^* and the shifted boundary conditions of Eq. (38), we should get the same result as the first-order unsplit method using D, and also the same results as RD splitting using D^*.

3.2.4. Results for linear reaction–diffusion problem

In the previous subsections, we have analyzed the effects of splitting on a linear reaction–diffusion problem using semi-discrete MPA. Results of this analysis indicate that if one uses an altered diffusion coefficient, along with possibly altered boundary conditions, the split methods will reproduce the answers

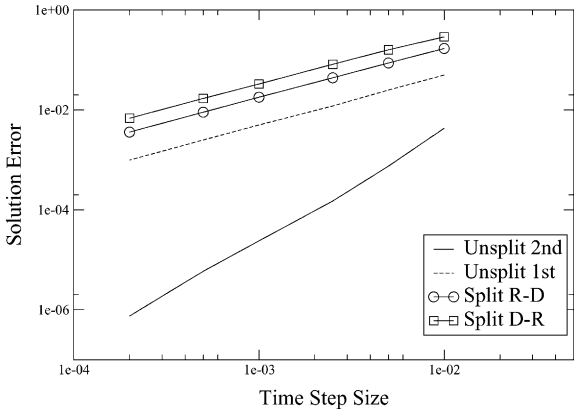

Fig. 9. Time step convergence of unsplit, RD split, and DR split formulations of the linear reaction–diffusion problem.

from an unsplit method. Here we demonstrate this computationally, and thus validate the MPA results of the previous subsections.

We consider the problem with $T(x,0) = 0$, $T_L = 1$, $T_R = 0$, $D = 1$, $\alpha = -20$, and $\Delta t = 0.01$, In Fig. 9 we show a time step convergence study verifying that the simple split methods are indeed first-order accurate. However, it is not apparent from this figure that either split method will get the correct steady-state solution using a large time step (i.e. $\alpha\Delta t \approx O(1)$). Fig. 10 shows the solutions themselves, as a function of time, at a particular point $(x = 0.1)$ for the different solution methods. At the chosen time step $\alpha\Delta t = 0.2$, the two split methods do not get the correct steady state solution. Furthermore, the two split methods are not equivalent even though their modified equations were identical. This demonstrates the importance of including boundary conditions in the error analysis. The solutions from the two split methods give no indication of error since they are stable and qualitatively correct.

In Fig. 11 we show the time history of the solution at the same particular point $(x = 0.1)$, for the first-order unsplit method, the RD splitting with the modified diffusion coefficient D^* (Eq. (34)), and the DR

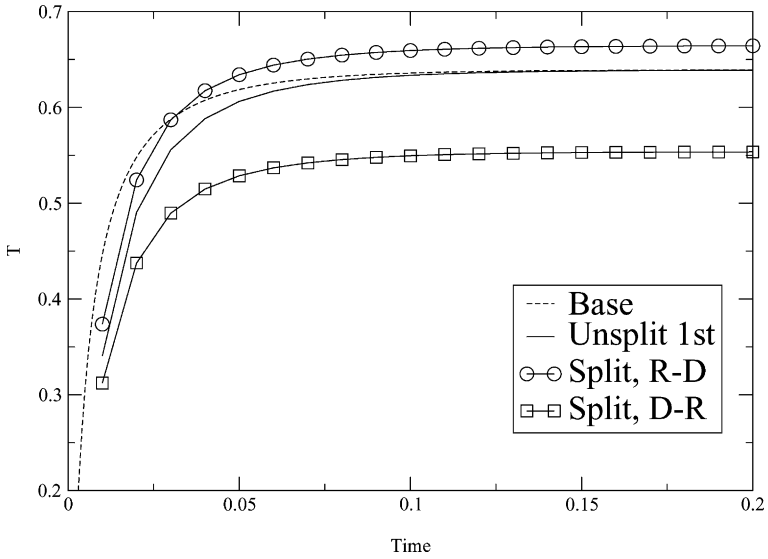

Fig. 10. Transient solutions at $X = 0.1$ for the linear reaction–diffusion problem.

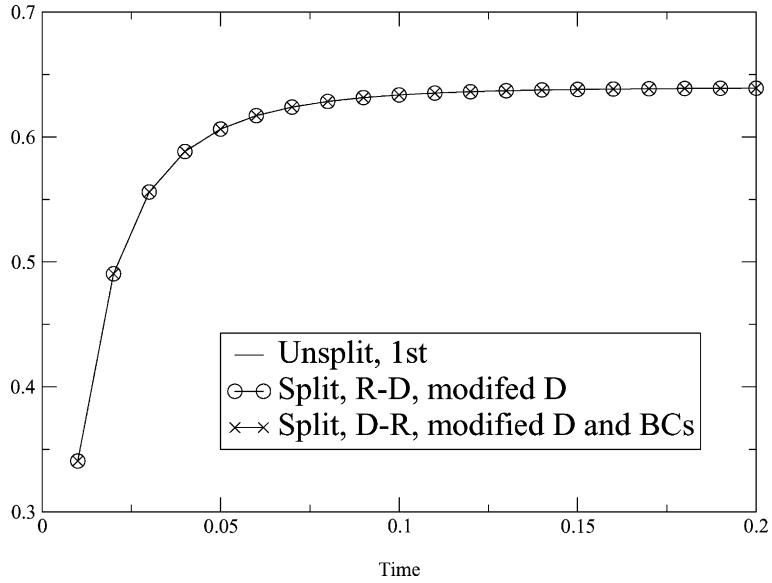

Fig. 11. Comparison of unsplit and split formulations of the linear reaction–diffusion problem with the corrected diffusion coefficient (D^*) and modified boundary conditions (in the DR split formulation only).

splitting with the modified diffusion coefficient and the altered boundary conditions (Eq. (38)). These three solutions are identical, confirming the validity of the MPA analysis of the splitting errors. Based on these results, it is evident that the solution from these first-order split methods can be interpreted as solutions from an unsplit method using an altered diffusion coefficient. The degree to which the diffusion coefficient is altered is proportional to the chosen time step normalized by a normal mode (fast) time scale, $\alpha\Delta t = \Delta t/\tau_{\text{reac}}$.

4. Accuracy results on coupled nonlinear PDE systems

In the previous section we demonstrated that linearization and/or splitting may have a serious impact on the accuracy of a numerical scheme. In addition, we demonstrated that second-order implicitly balanced time-integration methods can maintain accuracy at larger time steps, up to the dynamical time scales of the problem. The simplicity of the examples in Section 3 allows for clear understanding of the sources of inaccuracy. Here we illustrate the relevance of these results in more realistic applications of practical importance. The current section deals with multiple time scale nonlinear systems. The complex nature of these systems does not allow for the same level of analysis as was done in the previous section. However, we will point out the analogies in the behavior of the idealized and the more complex problems. We will also note commonalities among the examples in this section. In the present study we employ Jacobian-free Newton–Krylov methods to obtain implicitly balanced time integration. There are other approaches that could also be used.

4.1. Nonequilibrium radiation diffusion

Nonequilibrium radiation diffusion is an important process in many astrophysical problems [22], and in inertial confinement fusion [24,25]. The 1D model problem considered here has been studied previously in [26,19] and is an example of a strongly nonlinear reaction–diffusion system.

We consider the following 1D coupled system for the radiation energy E and the material temperature T,

$$\frac{\partial E}{\partial t} - \frac{\partial}{\partial x}\left(D_{\mathrm{r}}\frac{\partial E}{\partial x}\right) = \sigma_{\mathrm{a}}(T^4 - E), \tag{39}$$

$$\frac{\partial T}{\partial t} = -\sigma_{\mathrm{a}}(T^4 - E). \tag{40}$$

In these equations, material conduction and material motion are ignored; the physical basis for these approximations is discussed in [19]. Here $\sigma_{\mathrm{a}} = T^{-3}$ is the photon absorption cross-section. The flux-limited radiation diffusion coefficient, D_{r}, is given by

$$D_{\mathrm{r}}(T,E) = \frac{1}{\left(3\sigma_{\mathrm{a}} + \frac{1}{E}\left|\frac{\partial E}{\partial x}\right|\right)}. \tag{41}$$

In this set of equations (one PDE and one ODE), energy transport only occurs in the radiation field, while energy equilibration (the source term) couples the two fields.

The normal mode time scales in this problem arise from reaction (i.e., source term coupling) and from diffusion. The reaction time scale is $\tau_{\mathrm{reac}} \approx \sigma_{\mathrm{a}}^{-1}$. The dynamical time scale is the characteristic length of the thermal front divided by its propagation velocity [27]. This is analogous to the dynamical time scale in another well-known reaction diffusion problem, that of laminar flame propagation [28], as well as the idealized reaction–diffusion equation studied in Section 3.2. In all these three cases, the dynamical time scale results from a balance of a nonlinear reaction term with diffusion, which occurs in a thin ''reaction layer''. However, linearized (linearly implicit) and time-split methods have typically been used [22]. In [26,19] the phrase ''semi-implicit'' is used in place of linearly implicit. This is perhaps inadequate terminology, but we will continue to use it here for consistency. In the SI method, the two-component system remains coupled; however, D_{r}, σ_{a}, and T^4 are linearized using previous time level data, and the nonlinearities are not converged within a time step

$$\frac{E^{n+1} - E^n}{\Delta t} - \frac{\partial}{\partial x}\left(D_{\mathrm{r}}^n\frac{\partial E^{n+1}}{\partial x}\right) = \sigma_{\mathrm{a}}^n\left(T^{n+1}(T^n)^3 - E^{n+1}\right), \tag{42}$$

$$\frac{T^{n+1} - T^n}{\Delta t} = -\sigma_{\mathrm{a}}^n\left(T^{n+1}(T^n)^3 - E^{n+1}\right). \tag{43}$$

For comparison, we employ both a first-order (NK1) and second-order (NK2) accurate, nonlinear time integration method. The second-order method is based on a Crank–Nicolson approach:

$$\frac{E^{n+1} - E^n}{\Delta t} - \frac{1}{2}\frac{\partial}{\partial x}\left(D_{\mathrm{r}}^{n+1}\frac{\partial E^{n+1}}{\partial x}\right) - \frac{1}{2}\frac{\partial}{\partial x}\left(D_{\mathrm{r}}^{n}\frac{\partial E^{n}}{\partial x}\right) = \frac{1}{2}\sigma_{\mathrm{a}}^{n+1}\left((T^{n+1})^4 - E^{n+1}\right) + \frac{1}{2}\sigma_{\mathrm{a}}^{n}\left((T^{n})^4 - E^{n}\right), \tag{44}$$

$$\frac{T^{n+1} - T^n}{\Delta t} = -\frac{1}{2}\sigma_{\mathrm{a}}^{n+1}\left((T^{n+1})^4 - E^{n+1}\right) - \frac{1}{2}\sigma_{\mathrm{a}}^{n}\left((T^{n})^4 - E^{n}\right). \tag{45}$$

In this subsection we do not draw any conclusions on the effects of splitting, but only consider the effects of linearization and establish a connection to our results in Section 3.1. We establish that a first-order implicitly balanced method is more accurate than a first-order linearized method. We further establish that loss of design accuracy of the linearized method occurs when the first-order expansion of a linearized

coefficient fails to be adequate. Finally, we establish that a second-order implicitly balanced method can be integrated using a time step on the order of the dynamical time scale while remaining very accurate.

We will use problem 1 from [19], running with a fixed time step. The initial conditions are $E = 1.0 \times 10^{-5}$ and $T = E^{0.25}$. A Robin boundary condition for the radiation energy at $x = 0$ drives a thermal wave from left to right. In Fig. 12 we show results from a time step convergence study comparing the linearized method (SI) with the first-order (NK1) and second-order (NK2) nonlinear methods. All results are at time $t = 1$; the base solution was generated with the second-order method using a very small time step $\Delta t = 1.0 \times 10^{-4}$ (one percent of τ_{dyn}). The first observation is that the first-order nonlinear method is more accurate than the linearized method.

Next, we see that there is a range of time steps for which the SI method clearly does not achieve first-order time convergence (this is also true for NK1). In contrast, the NK2 method provides uniform second-order convergence throughout the range $\Delta t \in [5.0 \times 10^{-3}, 2.0 \times 10^{-2}]$.

This plot should be compared to Fig. 6 from Section 3.1. There are several quantities that are linearized in the SI method — (D_{r}, σ_{a}, T^4). Here we focus on the photon absorption cross-section, $\sigma_{\text{a}} = T^{-3}$, which is most analogous to $\alpha = (T^3 + a)^{-1}$ in the nonlinear ODE problem of Section 3.1. Its first-order Taylor series expansion in time is

$$\sigma_{\text{a}}^{n+1} \approx \sigma_{\text{a}}^{n} + \Delta t \frac{\mathrm{d}\sigma_{\text{a}}^{n}}{\mathrm{d}t}. \tag{46}$$

Fig. 12 shows that, at the smaller time step, the SI method achieves first-order convergence, but at the larger time step size it does not. In Figs. 13 and 14 we show plots of σ_{a}^{n+1}, σ_{a}^{n}, and $\sigma_{\text{a}}^{n} + \Delta t(\mathrm{d}\sigma_{\text{a}}^{n}/\mathrm{d}t)$, for time step sizes of 1.0×10^{-3} and 5.0×10^{-3}, respectively. All quantities are measured at the thermal front at time $t = 1$. Fig. 13 shows that at the (smaller) time step of 1.0×10^{-3}, the first-order Taylor expansion of σ_{a} is a good approximation for the new time value; we should expect to find first-order convergence and Fig. 12 confirms this. In contrast, at the (larger) time step of 5.0×10^{-3} Fig. 14 shows that the first-order Taylor expansion is not a good approximation for the new time value and so we should not expect first-order convergence. Again, Fig. 12 confirms this conclusion.

For this problem the "average" dynamical time scale is $\tau_{\text{dyn}} \approx 0.015$, while the reaction (source term) time scale is $\tau_{\text{reac}} \approx 0.0005$. As seen in Fig. 12, the second-order nonlinear method achieves design accuracy at $\Delta t \approx \tau_{\text{dyn}}$, while the linearized (SI) method does not achieve design accuracy until $\Delta t \approx \tau_{\text{reac}}$.

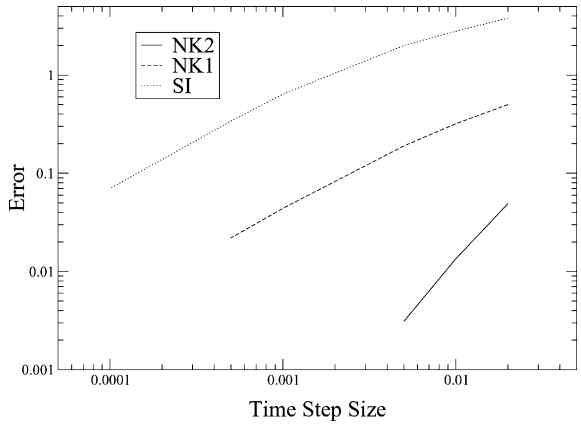

Fig. 12. Time step convergence study of the linearized method (SI), the first-order nonlinear method (NK1) and the second-order nonlinear method (NK2) for the nonequilibrium radiation–diffusion problem.

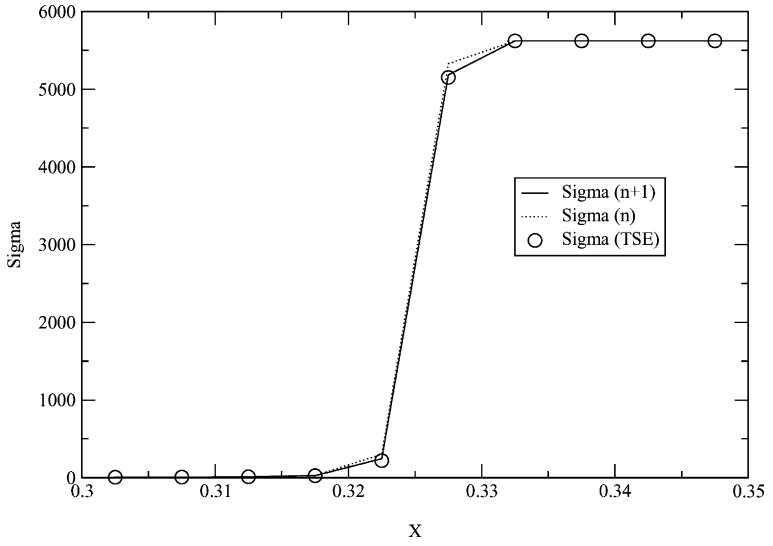

Fig. 13. Plot of σ_a^{n+1} (Sigma $(n+1)$), σ_a^n (Sigma (n)), and $\sigma_a^n + \Delta t \frac{d\sigma_a^n}{dt}$ (Sigma TSE) at the location of the thermal front for $\Delta t = 1 \times 10^{-3}$.

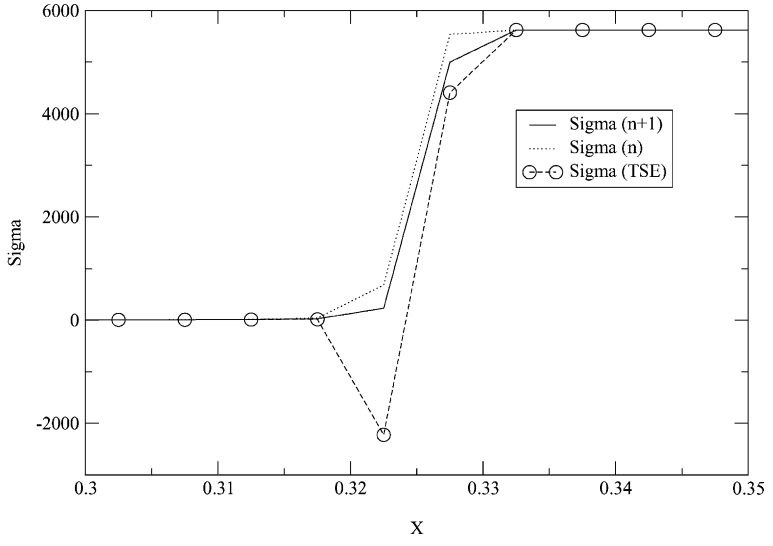

Fig. 14. Plot of σ_a^{n+1} (Sigma $(n+1)$), σ_a^n (Sigma (n)), and $\sigma_a^n + \Delta t \frac{d\sigma_a^n}{dt}$ (Sigma TSE) at the location of the thermal front for $\Delta t = 5 \times 10^{-3}$.

Finally, a method that is less than first-order accurate in time can rapidly deviate from the proper solution trajectory, diminishing the total problem time for which the simulation is predictive. Fig. 15 displays the results of a time step convergence analysis for a first (NK1) and a second-order (NK2) nonlinear method and for the SI method. Results are shown at two points in time in a log-linear scale. The build up of error in the SI method from time = 0.4 to time = 1.0 is dramatic for time steps, where SI does not achieve first-order convergence ($\approx \Delta t = 1 \times 10^{-2}$). Examining the actual solution at two different times in Fig. 16 for $\Delta t = 1 \times 10^{-2}$, we see the SI method drifting further from the "base" solution as time progresses. This results in a loss of accuracy, although the solution looks qualitatively correct. Recall that at time = 1.0, we

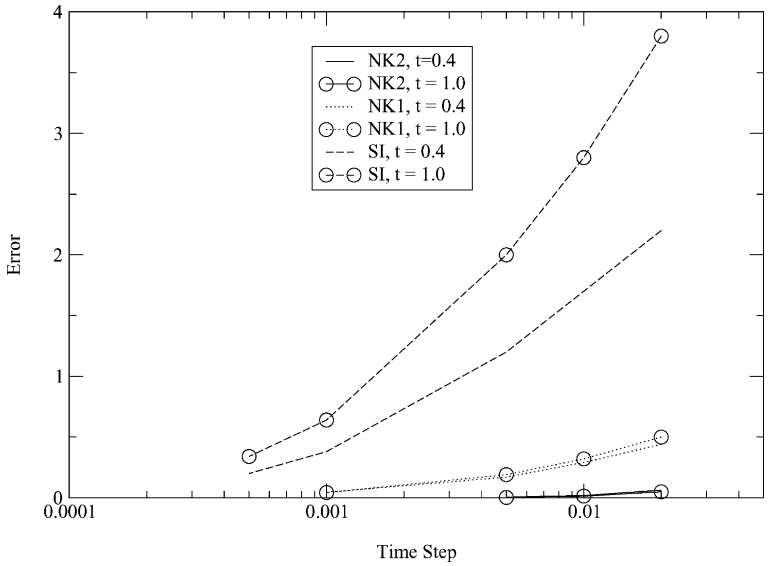

Fig. 15. Time convergence study for the first-order (NK1) and second-order (NK2) implicitly balanced methods and the SI method at two different points in time ($t = 0.4,\ 1.0$).

have only taken 100 time steps. The second-order implicitly balanced method is clearly able to retain a predictive capability at the same time step size. If one reduces the SI time step to $\Delta t = 1 \times 10^{-3}$ then the solution at time = 0.4 (not shown) looks much better, but by time = 3.0 (not shown), one again observes significant drift.

There are many similarities between the analysis and results of Section 3.1 and these radiation–diffusion results. A more detailed analysis of this problem, including MEA and an analysis of the effects of splitting are left to a future study. Further study of error propagation in time, and of how the number of time steps and the error accumulation per time step determine the predictivity of a solution is also desirable. Also, the issue of CPU effort for a given accuracy has been addressed for this problem in [19], and the second-order implicitly balanced approach was shown to have the distinct advantage.

4.2. Reduced MHD equations

The equations of magnetohydrodynamics (MHD) are used to model phenomena in controlled thermonuclear fusion, space physics, and astrophysics [29]. To illustrate the difficulties in solving these equations, we consider a simplified 2D system that retains a classic stiff wave structure with multiple time scales. The 2D (x–y plane) reduced MHD (RMHD) equation system [30–32], in Alfvénic units ($\tau_A = L_y/v_A$ is the Alfvén time, and $v_A = B_0$ is the Alfvén speed) is:

$$\nabla^2 \Phi = \omega, \tag{47}$$

$$\frac{\partial \Psi}{\partial t} + (\vec{v} \cdot \nabla - \eta \nabla^2)\Psi + E_0 = 0, \tag{48}$$

$$\frac{\partial \omega}{\partial t} + (\vec{v} \cdot \nabla - v \nabla^2)\omega + \dot{S}_\omega = \vec{B} \cdot \nabla J. \tag{49}$$

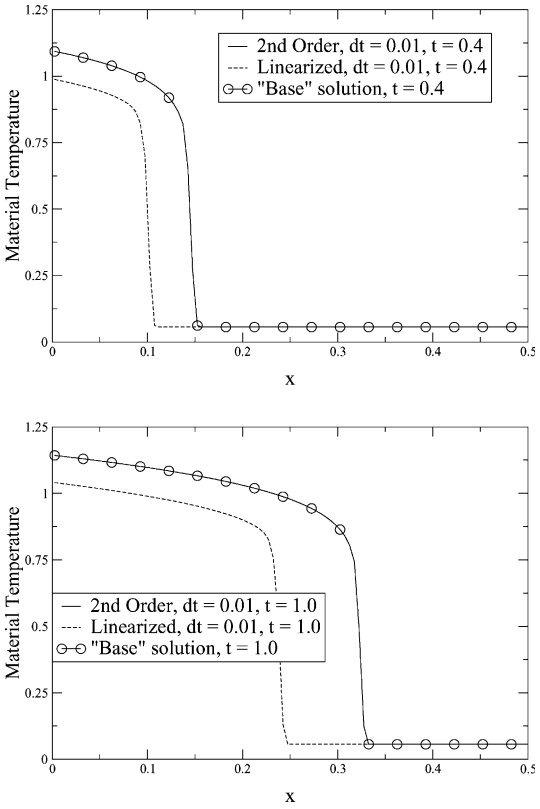

Fig. 16. Thermal front propagation in the nonequilibrium radiation–diffusion problem using the second-order implicitly balanced method (2nd) and the SI method (linearized) at two different times ($t = 0.4,\ 1.0$).

Here Φ is the $x - y$ velocity stream function (i.e., $\vec{v} = \vec{z} \times \nabla\Phi$), $\omega = \vec{z} \cdot \nabla \times \vec{v}$ is the vorticity in the x–y plane, Ψ is the flux function, $\vec{B} = \vec{z} \times \nabla\Psi$, and $J = \nabla^2\Psi$ is the current in the ignorable direction (z). The source terms E_0 (the applied electric field in the z direction) and $\dot{S}_\omega$ have been included to balance the decay of the ideal equilibrium due to transport. The transport parameters are the kinematic viscosity ν and the resistivity η, which are both assumed constant. An implicitly balanced algorithm for this equation system is documented in [20].

The normal mode time scales in this system come from Alfvén wave propagation (fast), diffusion (slow), and advection. Dynamical time scales of interest arise from resistive instabilities (such as tearing modes [33,29]). These are much slower than the Alfvén wave propagation time scale making explicit solution methods inefficient. However, as in other problems described in this paper, linearization and splitting are typically used to make the implicit solution methods more tractable. To investigate the effects of these simplifications, we focus on a classical tearing mode problem on a rectangular 2D domain $L_x \times L_y$. The problem is initialized with a current sheet

$$\Psi_0(x, y) = \frac{1}{\lambda} \ln \left[\cosh \lambda \left(y - \frac{1}{2} \right) \right].$$

We set $\Phi_0 = \omega_0 = 0$. The parameter λ determines the inverse of the characteristic width of the current sheet and also the tearing mode growth rate – i.e., the larger λ, the narrower the current sheet and the larger the tearing growth rate. The dynamical time scale, which is the inverse of the growth rate, results from a

balance between the resistive diffusion and the Alfvén wave propagation [33,29]. It has the functional form $\gamma = (\tau_A \tau_D)^{-1/2}$ in units of s^{-1}. Here, τ_D is the resistive diffusion time scale; typically $\tau_D \gg \tau_A$. Thus, the growth rate is fast compared to resistive diffusion, but slow compared to Alfvén wave propagation. The tearing mode is excited by a perturbation of the flux

$$\delta\Psi = 10^{-3}\sin(\pi y)\cos\left(\frac{2\pi}{L_x}x\right).$$

The simulation parameters are $L_x = 3$, $L_y = 1$, $\lambda = 5$, and $\eta = \nu = 10^{-3}$. For this choice of parameters, the tearing mode growth rate is $\gamma = 0.0435\tau_A^{-1}$ [20].

To demonstrate the accuracy advantage of an implicitly balanced solution of Eqs. (47)–(49), we consider four time discretizations:

1. A first-order balanced scheme (backward Euler).
2. A second-order balanced Crank–Nicolson difference scheme:

$$\nabla^2\Phi^{n+1} = \omega^{n+1}, \tag{50}$$

$$\frac{\Psi^{n+1}-\Psi^n}{\Delta t} + [\vec{v}\cdot\nabla\Psi]^{n+(1/2)} - \eta\nabla^2\Psi^{n+(1/2)} = -E_0, \tag{51}$$

$$\frac{\omega^{n+1}-\omega^n}{\Delta t} + [\vec{v}\cdot\nabla\omega]^{n+(1/2)} - \nu\nabla^2\omega^{n+(1/2)} = [\vec{B}\cdot\nabla J]^{n+(1/2)} - \dot{S}_\omega, \tag{52}$$

   where quantities at the $(n+1/2)$-time level are calculated as $\xi^{n+(1/2)} = (\xi^{n+1}+\xi^n)/2$.
3. A split scheme where resistive diffusion is updated in a split step

$$\nabla^2\Phi^{n+1} = \omega^{n+1}, \tag{53}$$

$$\frac{\Psi^{\star}-\Psi^n}{\Delta t} + [\vec{v}\cdot\nabla\Psi]^{(\star+n)/2} = 0, \tag{54}$$

$$\frac{\omega^{n+1}-\omega^n}{\Delta t} + [\vec{v}\cdot\nabla\omega]^{n+(1/2)} - \nu\nabla^2\omega^{n+(1/2)} = [\vec{B}\cdot\nabla J]^{(\star+n)/2} - \dot{S}_\omega, \tag{55}$$

$$\frac{\Psi^{n+1}-\Psi^{\star}}{\Delta t} - \eta\nabla^2\Psi^{n+1} = -E_0. \tag{56}$$

   The split step (denoted by ☆) makes this discretization first-order accurate in time.
4. With a linearized scheme in which $[\vec{B}\cdot\nabla J]^{n+1/2}$ is approximated in Eq. (52) by $\vec{B}^n\cdot\nabla J^{n+1/2}$, similar to how one derives Harned–Kerner SI operators for MHD waves [34].

In the typical MHD SI method [34] there is both linearization and splitting. We consider the effects separately here. As noted earlier, the tearing mode is a balance between resistive diffusion and Alfvén wave propagation. We expect that approaches 3 and 4 above will not be able to obtain this balance accurately in simulations using large time steps, while approach 1 will suffer from standard first-order time discretization error.

We compare the numerical error of the four schemes above in the tearing problem, evaluated at a particular time $T_f = 60\tau_A$, as a function of $\gamma\Delta t$. Results are shown on two grids, 64×64 and 256×256. Numerical error is measured by $||\vec{\Psi}-\vec{\Psi}_{\text{base}}||_2$, where $\vec{\Psi}$ is the poloidal flux solution vector and $\vec{\Psi}_{\text{base}}$ is a

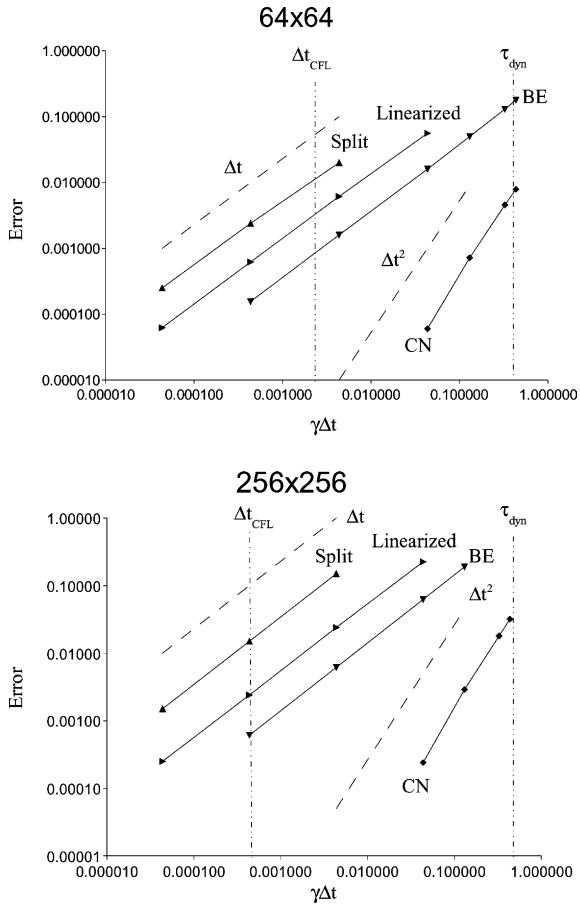

Fig. 17. Comparison of the numerical error resulting from the first (BE) and second (CN) order implicitly balanced approaches, the split method, and the linearized method using the RMHD model on a tearing mode problem in 64×64 and 256×256 grids. Dashed lines are test scalings for first (Δt) and second (Δt^2) order convergence.

"base" solution obtained with $\Delta t = \Delta t_{\mathrm{CFL}}$ (i.e., the explicit time step required for stability of Alfvén waves) using the second-order balanced method. The results are presented in Fig. 17.

To summarize these results:

1. The second-order balanced method 2 shows true second-order convergence. Either approximation – splitting or linearizing at least one term – degrades accuracy to first order. An MEA of methods 3 and 4 above should uncover a new first-order error, and it should scale as $\Delta t/\tau_{\mathrm{A}}$. These details are left for future work.
2. The second-order balanced approach allows time steps of the order of the dynamical time scale ($\gamma\Delta t \sim 1/2$) without compromising accuracy; the other approaches are required to closely follow the explicit Alfvén wave CFL time step (a normal mode time scale) for comparable accuracy (although not for stability, since all approaches are numerically stable). Consequently, for the same error level, the second-order accurate scheme allows implicit time steps orders of magnitude larger than either the split or the linearized scheme.

It is interesting to note that the process of splitting the resistive diffusion update generates more error than linearizing the body force. MEA should provide insight into this. In addition, in [20] it was demonstrated that,

for the same level of accuracy, a second-order implicitly balanced method can be close to an order of magnitude faster (in terms of overall CPU) than an explicit method for this stiff wave MHD problem.

4.3. Shallow water equations

The shallow water equations are a 2D system of conservation laws that can be used to model many problems in geophysical fluid dynamics. Like the MHD equations in the previous subsection, this is a classic stiff wave system where the dynamical time scales of interest are often significantly slower than the gravity wave time scale. An efficient, second order, implicitly balanced method for this equation system is documented in [21]. Here we perform an approximate (semi-discrete) MEA (similar to that performed on the linear reaction diffusion problem in Section 3.2), which illuminates the difference between a first-order implicitly balanced solution method and a classic SI method for the shallow water equations.

As previously seen, an implicitly balanced algorithm has all terms evaluated at the same time level, and the nonlinearities in the equations are iterated to convergence before moving to the next time step. In contrast, the SI method considered here linearizes the potential energy gradient term, uses fully explicit momentum fluxes, and does not iterate to nonlinear consistency. The splitting of the time step with the variables at different time levels results in differences in the modified equations, as will be shown.

The shallow-water equations with rotation can be written in conservation form in two dimensions as:

$$\frac{\partial h}{\partial t} + \nabla \cdot (\vec{v}h) = 0, \tag{57}$$

$$\frac{\partial \vec{v}h}{\partial t} + \nabla \cdot (\vec{v}h \otimes \vec{v}) + \frac{1}{2} g \nabla h^2 - f\vec{z} \times (\vec{v}h - \vec{v}_{bg}h) = 0. \tag{58}$$

Here h is the height of the fluid, $\vec{v}$ is the fluid velocity ($\vec{v} = u\hat{x} + v\hat{y}$), g is the gravitational acceleration, f is the Coriolis parameter (frequency), and $\vec{v}_{bg}$ is the background wind velocity, which is an external forcing function. The gravity wave speed is $\sqrt{gh}$.

The semi-discrete approximations of Eqs. (57) and (58) for a first-order implicitly balanced algorithm are

$$\frac{h^{n+1} - h^n}{\Delta t} + \nabla \cdot (\vec{v}h)^{n+1} = 0, \tag{59}$$

$$\frac{(\vec{v}h)^{n+1} - (\vec{v}h)^n}{\Delta t} + \nabla \cdot (\vec{v}h^{n+1} \otimes \vec{v}^{n+1}) + \frac{1}{2} g \nabla (h^{n+1})^2 - f\vec{z} \times (\vec{v}h^{n+1} - \vec{v}_{bg}h^{n+1}) = 0. \tag{60}$$

Again, the spatial discretizations have not been included since the current analysis focuses on the temporal errors introduced by splitting, and the resolution is chosen to ensure that the spatial errors are small. The corresponding modified equations are

$$\frac{\partial h}{\partial t} + \nabla \cdot (\vec{v}h^{n+1}) = \frac{\Delta t}{2} \frac{\partial^2 h}{\partial t^2} + \mathrm{O}(\Delta t^2), \tag{61}$$

$$\frac{\partial (\vec{v}h)}{\partial t} + \nabla \cdot (\vec{v}h^{n+1} \otimes \vec{v}^{n+1}) + \frac{1}{2} g \nabla (h^{n+1})^2 - f\vec{z} \times (\vec{v}h^{n+1} - \vec{v}_{bg}h^{n+1}) = \frac{\Delta t}{2} \frac{\partial^2 (\vec{v}h)}{\partial t^2} + \mathrm{O}(\Delta t^2). \tag{62}$$

The semi-discrete equations of the SI algorithm are

$$\frac{h^{n+1} - h^n}{\Delta t} + \nabla \cdot (\vec{v}h)^{n+1} = 0, \tag{63}$$

$$\frac{(\vec{v}h)^{n+1}-(\vec{v}h)^{n}}{\Delta t}+\nabla\cdot(\vec{v}h^{n}\otimes\vec{v}^{n})+\frac{1}{2}gh^{n}\nabla h^{n+1}-f\vec{z}\times(\vec{v}h^{n+1}-\vec{v}_{bg}h^{n+1})=0. \tag{64}$$

Here the advection terms are explicit and the potential energy gradient has been linearized. In the standard SI method, $(\vec{v}h)^{n+1}$ is evaluated from Eq. (64) and substituted into Eq. (63), leading to a linear scalar parabolic equation for h^{n+1}. The corresponding modified equations for the SI algorithm are

$$\frac{\partial h}{\partial t}+\nabla\cdot(\vec{v}h^{n+1})=\frac{\Delta t}{2}\frac{\partial^2 h}{\partial t^2}+\mathrm{O}(\Delta t^2), \tag{65}$$

$$\begin{aligned}&\frac{\partial(\vec{v}h)}{\partial t}+\nabla\cdot(\vec{v}h^{n+1}\otimes\vec{v}^{n+1})+\frac{1}{2}g\nabla(h^{n+1})^2-f\vec{z}\times(\vec{v}h^{n+1}-\vec{v}_{bg}h^{n+1})\\&\quad=\frac{\Delta t}{2}\frac{\partial^2(\vec{v}h)}{\partial t^2}+\nabla\cdot(\vec{v}h^{n+1}\otimes\vec{v}^{n+1})-\nabla\cdot\left(\left\{\vec{v}h^{n+1}-\Delta t\frac{\partial\vec{v}h}{\partial t}\right\}\otimes\left\{\vec{v}^{n+1}-\Delta t\left[\frac{1}{h}\frac{\partial\vec{v}h}{\partial t}-\frac{\vec{v}h}{h^2}\frac{\partial h}{\partial t}\right]\right\}\right)\\&\qquad+\Delta tg\nabla h\frac{\partial h}{\partial t}+\mathrm{O}(\Delta t^2).\end{aligned} \tag{66}$$

Comparing the modified equations of the SI method to those of the implicitly balanced method, we see that in addition to the errors that come from the time derivative, we now have additional terms arising from the explicit advection and from the linearized body forces. This is similar to the case of splitting on the linear reaction diffusion problem in Section 3.2. Indeed, the combined body force term in the modified momentum equation can be interpreted as having an altered gravity wave speed $\sqrt{g(h+\Delta t\frac{\partial h}{\partial t})}$.

The initial conditions for the shallow water test problem are given by the following two equations, which define tangential velocity (v_t) and the height (h) as a function of radius r. These represent a vortex in the center of the computational domain, assumed square and with sides 2.0×10^6 m.

$$v_t(r)=\frac{r}{8.0\times10^3}\frac{\exp\left(-5.5\times10^{-6}\left[\frac{r}{8.0\times10^4}\right]^6\right)}{1+\left[\frac{r}{8.0\times10^4}\right]^2} \tag{67}$$

$$\frac{\partial h(r)}{\partial r}=\frac{1}{9.8}\left(\frac{v_t^2}{r}+5.0\times10^{-5}v_t\right). \tag{68}$$

Here $h(\infty)=1.0\times10^3$ m, gravity is 9.8 ms^{-2}, the Coriolis frequency is 5.0×10^{-5} s^{-1}, the background wind blows towards the north-east (diagonally) at 1.5 ms^{-1}, and the problem time is 14 days.

In analogy to our study of the simpler equations in Section 3, we compare the solutions from a first-order implicitly balanced method (solution A), a first-order implicitly balanced solution of the SI modified equations that neglects $(\Delta t/2)(\partial^2 h/\partial t^2)$ in Eq. (65) $(\Delta t/2)(\partial^2(\vec{v}h)/\partial t^2)$ in Eq. (66) and $\mathrm{O}(\Delta t^2)$ in both (solution B), and the SI solution itself (solution C). In the semi-discrete MEA we have ignored errors associated with spatial discretization. Assuming that these spatial errors are relatively smaller, we would expect that solutions B and C above will be equivalent, and different from solution A. Indeed, Fig. 18 shows that the solutions B and C are nearly identical, and differ from solution A, once again validating the MEA.

The time step convergence plot in Fig. 19 shows that for the SI method to get approximately the same accuracy as the second-order implicitly balanced method using $\Delta t\approx0.5\tau_{\mathrm{dyn}}$, the SI method must use a time

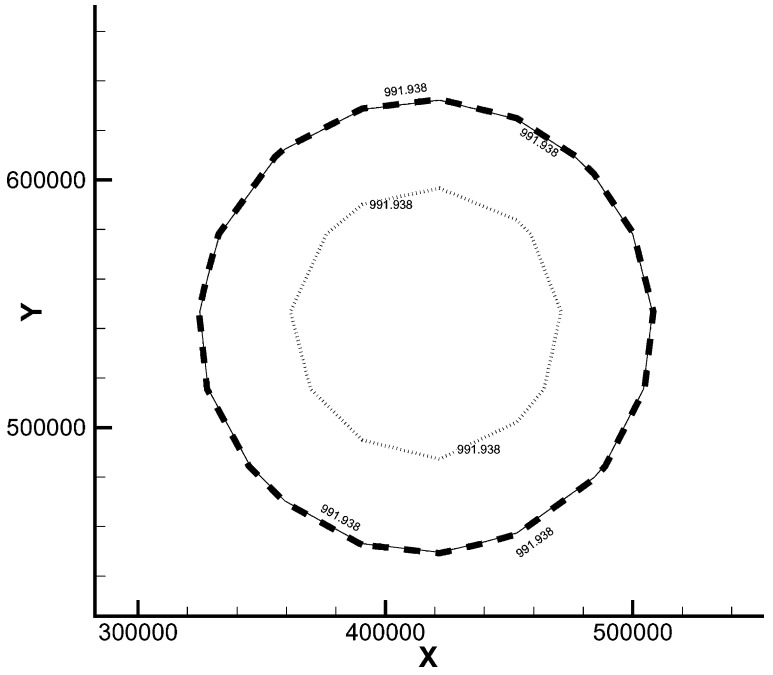

Fig. 18. Approximate MEA verification in the travelling vortex problem. Contour of constant height on a 64×64 grid with (1) a 1st order implicitly balanced method (dotted), (2) an implicitly balanced solution of the SIs modified equations (solid), and (3) a SI method (dashed).

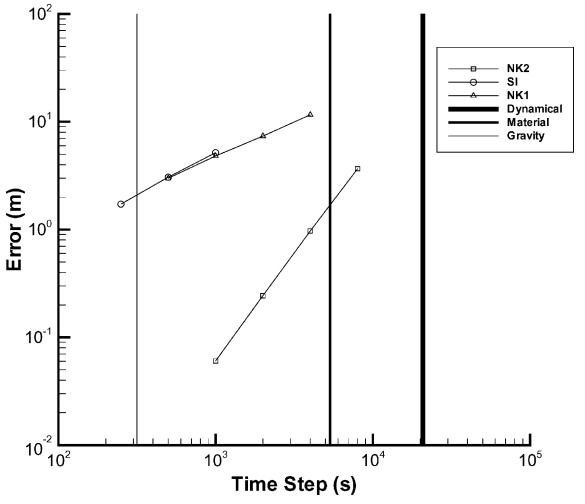

Fig. 19. Time step convergence study on a 64×64 grid using the travelling vortex problem.

step near the stiff wave CFL (i.e., ensuring that gravity waves are stable in an explicit approximation). This is similar to what we observed in the split solution of the MHD problem in the previous subsection. This is also consistent with the results of splitting on the linear reaction–diffusion problem in Section 3.2. In all

cases, when linearization and splitting are used, the linearized split method must resolve the stiff time scales involved in the balance in order to attain comparable accuracy to an implicitly balanced method. In addition, in contrast to the problems in the previous two subsections, we see that in this problem the SI method has comparable accuracy to the first-order implicitly balanced method. Thus, for this set of conditions, the truncation terms

$$\frac{\Delta t}{2}\frac{\partial^2 h}{\partial t^2} \quad \text{and} \quad \frac{\Delta t}{2}\frac{\partial^2(\vec{v}h)}{\partial t^2}$$

dominate over the additional truncation terms resulting from splitting and linearization. Because the SI method has a stability limit associated with the (advective) Courant condition, the first-order implicitly balanced method can run at a larger time step. Finally, in [21] the second-order implicitly balanced method was shown to be more efficient than the SI method for a given level of accuracy.

5. Conclusions

In this paper, we have considered numerical time integration on a class of problems in which the dynamical time scales arise from an asymptotic balance of normal mode time scales. It is desirable in such problems to resolve only the slow dynamical time scale, overstepping the fast normal mode time scales. We have shown that this can be achieved using implicitly balanced methods. We have further considered alternate, approximate solution methods that employ splitting and/or linearization. The questions we are interested in asking in this study are related to accuracy.

To answer these questions, we have used modified equation analysis (MEA). In Section 3, MEA was applied to a simple nonlinear ODE and a simple linear reaction–diffusion PDE. Analytical insight on the effects of linearization and splitting was obtained. It was shown that:

- Linearization is particularly deleterious when very nonlinear coefficients are present, and may result in loss of first-order accuracy and in stalling of the numerical error (i.e., the error behaves as $O(\Delta t^{\beta})$, with $\beta < 1$, even if the algorithm is formally of first order) for sufficiently large time steps (i.e., larger than the characteristic rate of change of the nonlinear coefficients). In contrast, second-order, implicitly balanced numerical algorithms maintain second-order convergence even when time steps comparable to the dynamical time scale of the problem are used.
- Time splitting techniques effectively modify the transport coefficients of a problem, as well as the boundary conditions, and result in incorrect (transient and steady-state) solutions when time steps exceeding the normal mode time scales are used. For the linear PDE considered, MPA was able to provide an exact prescription for altering the diffusion coefficient and boundary conditions, so as to allow the splitting methods to produce the identical result as an unsplit method.

We extended our study to more realistic applications in Section 4. In particular, we described problems with a propagating thermal front in a 1D nonequilibrium radiation–diffusion model, a resistive instability (tearing mode) in a 2D reduced MHD model, and a traveling vortex in the 2D shallow water equations. Accuracy comparisons were made among split, linearized, and implicitly balanced implementations of the governing equations for each of these applications. Although each of these is far more complex than the idealized problems of Section 3, we were able to identify similar effects due to splitting and/or linearization in each of the realistic applications. In particular, it was shown that linearized and split algorithms must resolve the time scales of the fastest normal modes if they are to provide comparable numerical accuracy to the second order implicitly balanced approach using time steps comparable to the dynamical time scale.

While this study has focused on accuracy, the issue of efficiency has been addressed in [19–21] for all three problems considered in Section 4. Thus, we conclude that second-order implicitly balanced algorithms

provide a viable approach for time integration of problems with dynamical time scales much longer than existing normal modes, both from the efficiency standpoint (e.g., if properly preconditioned Newton–Krylov techniques are employed [19–21]) and from the accuracy standpoint.

Acknowledgements

We gratefully acknowledge discussions with R.B. Lowrie, W. J. Rider, J.N. Shadid, and P.K. Smolarkiewicz. This work was supported by the Laboratory Directed Research and Development Program. Los Alamos National Laboratory is operated by the U.S. Department of Energy under contract W-7405-ENG-36. L.C. has been supported by a Director-funded Postdoctoral Fellowship at Los Alamos National Laboratory.

References

[1] J. Brackbill, B. Cohen, Multiple Time Scales, Academic Press, Orlando, 1985.
[2] P.N. Brown, Y. Saad, Hybrid Krylov methods for nonlinear systems of equations, SIAM J. Sci. Stat. Comput. 11 (1990) 450–481.
[3] T.F. Chan, K.R. Jackson, Nonlinearly preconditioned Krylov subspace methods for discrete Newton algorithms, SIAM J. Sci. Stat. Comput. 5 (1984) 533–542.
[4] G. Strang, On the construction and comparison of difference schemes, SIAM J. Numer. Anal. 5 (1968) 506–517.
[5] G. Browning, H.-O. Kriess, Splitting methods for problems with different time scales, Mon. Weather Rev. 122 (1994) 2614–2622.
[6] B. Sportisse, An analysis of operator splitting techniques in the stiff case, J. Comp. Phys. 161 (2000) 140–168.
[7] C. Hirt, Heuristic stability theory for finite difference equations, J. Comp. Phys. 2 (1968) 339–355.
[8] R. Warming, B. Hyett, The modified equation approach to the stability and accuracy analysis of finite-difference methods, J. Comp. Phys. 14 (1974) 159–179.
[9] D.F. Griffiths, J. Sanz-Serna, On the scope of the method of modified equations, SIAM J. Sci. Stat. Comput. 3 (1986) 994–1008.
[10] J.N. Shadid, C.C. Ober, R.P. Pawlowski, D.L. Ropp, Studies on Solution Methods for Nonlinear, Multiple-Time-Scale, PDE Simulations: examples from diffusion reaction systems, in: Proc. of Seventh Copper Mountain Conference on Iterative Methods, Copper Mountain, Colorado, March 2002.
[11] S.-C. Chang, A critical analysis of the modified equation technique of Warming and Hyett, J. Comp. Phys. 86 (1990) 107–126.
[12] P.K. Smolarkiewicz, L.G. Margolin, MPDATA: a finite difference solver for geophysical flows, J. Comp. Phys. 140 (1998) 459–480.
[13] P.K. Smolarkiewicz, L.G. Margolin, On forward-in-time differencing for fluids: extension to a curvilinear framwork, Mon. Weather Rev. 121 (1993) 1847–1859.
[14] R.B. Lowrie, J.E. Morel, Methods for hyperbolic systems with stiff relaxation, Int. J. Numer. Methods Fluids 40 (2002) 413–423.
[15] D.A. Jones, L.G. Margolin, E.S. Titi, On the effectiveness of the approximate inertial manifold, Theor. Comp. Fluid Dyn. 7 (1995) 243–260.
[16] D.A. Jones, L.G. Margolin, A.C. Poje, Enslaved finite difference schemes for nonlinear dissipative PDEs, Numer. Methods PDEs 12 (1996) 13–40.
[17] A.C. Poje, D.A. Jones, L.G. Margolin, Enslaved finite difference approximations for quasi-geostrophic shallow flows, Physica D 98 (1996) 559–573.
[18] Y. Saad, Iterative Methods for Sparse Linear Systems, PWS Publishing Company, Boston, 1996.
[19] D.A. Knoll, W.J. Rider, G.L. Olson, Nonlinear convergence, accuracy, and time step control in non-equilibrium radiation diffusion, J. Quant. Spectrosc. Radiat. Transfer 70 (2001) 25–36.
[20] L. Chacon, D.A. Knoll, J.M. Finn, An implicit nonlinear reduced resistive MHD solver, J. Comput. Phys. 178 (2002) 15–36.
[21] V. Mousseau, D.A. Knoll, J. Reisner, An implicit nonlinearly consistent method for the two-dimensional shallow-water equations with Coriolis force, Mon. Weather Rev. 130 (2002) 2611–2625.
[22] R.L. Bowers, J.R. Wilson, Numerical Modeling in Applied Physics and Astrophysics, Jones and Bartlett, Boston Publishers, 1991.
[23] E.S. Oran, J.P. Boris, Numerical Simulation of Reactive Flow, Elsevier, New York, 1987.
[24] C. Baldwin, P.N. Brown, R. Falgout, F. Graziani, J. Jones, Iterative linear solvers in a 2d radiation-hydrodynamics code: methods and performance, J. Comput. Phys. 154 (1999) 1–40.
[25] A.M. Winslow, Multifrequency-gray method for radiation diffusion with Compton scattering, J. Comput. Phys. 117 (1995) 262–273.

[26] D.A. Knoll, W.J. Rider, G.L. Olson, An efficient nonlinear solution method for non-equilibrium radiation diffusion, J. Quant. Spectrosc. Radiat. Transfer 63 (1999) 15–29.
[27] W.J. Rider, D.A. Knoll, Time step size selection for radiation diffusion calculations, J. Comput. Phys. 152 (1999) 790–795.
[28] F.A. Williams, Combustion Theory, Addison-Wesley Publishers, Reading, Mass, 1985.
[29] D. Biskamp, Nonlinear Magnetohydrodynamics, Cambridge University Press, Cambridge, 1993.
[30] H.R. Strauss, Nonlinear, 3-dimensional magnetohydrodynamics of noncircular tokamaks, Phys. Fluids 19 (1) (1976) 134–140.
[31] J.F. Drake, T.M. Antonsen, Nonlinear reduced fluid equations for toroidal plasmas, Phys. Fluids 27 (4) (1984) 898–908.
[32] R.D. Hazeltine, M. Kotschenreuther, P.J. Morrison, A four-field model for tokamak plasma dynamics, Phys. Fluids 28 (8) (1985) 2466–2477.
[33] H.P. Furth, J. Killeen, M.N. Rosenbluth, Finite-resistivity instabilities of a sheet pinch, Phys. Fluids 4 (1963) 459–484.
[34] D. Harned, W. Kerner, Semi-implicit method for three-dimensional compressible magnetohydrodynamic simulation, J. Comp. Phys. 60 (1985) 62–75.